

# Discovery of fluorotelomer sulfones in the blubber of Greenland Killer Whales (*Orcinus orca*)

Mélanie Z. Lauria,<sup>1\*</sup> Xiaodi Shi,<sup>1</sup> Faiz Haque,<sup>1, 2</sup> Merle Plassmann,<sup>1</sup> Anna Roos,<sup>3, 4</sup> Malene Simon,<sup>4</sup> Jonathan P. Benskin,<sup>#1\*</sup> and Karl J. Jobst<sup>#5\*</sup>

<sup>1</sup>Department of Environmental Science, Stockholm University, Svante Arrhenius Väg 8, 10691 Stockholm, Sweden

<sup>2</sup>Department of Materials and Environmental Chemistry, Stockholm University, Svante Arrhenius Väg 16, 106 91, Stockholm, Sweden

<sup>3</sup>Department of Environmental Research and Monitoring, Swedish Museum of Natural History, 104 05 Stockholm, Sweden

<sup>4</sup>Greenland Climate Research Centre, Greenland Institute of Natural Resources, 3900 Nuuk, Greenland

<sup>5</sup>Department of Chemistry, Memorial University of Newfoundland, 45 Arctic Ave., St. John's, Canada A1C 5S7

<sup>#</sup>JPB and KJ contributed equally and share the last authorship.

\*Corresponding authors:

[Melanie.Lauria@aces.su.se](mailto:Melanie.Lauria@aces.su.se)

[Jon.Benskin@aces.su.se](mailto:Jon.Benskin@aces.su.se)

[kjobst@mun.ca](mailto:kjobst@mun.ca)

## Abstract

Most known per- and polyfluoroalkyl substances (PFAS) bioaccumulate by binding to proteins or partitioning to phospholipids, leading to their prevalence in liver and blood. As a result, efforts to improve PFAS exposure estimates by identifying novel bioaccumulative substances, have focused on these tissues. However, the recent discovery of high concentrations of unidentified extractable organofluorine (EOF) in the blubber of a killer whale (*Orcinus orca*) from Greenland suggests that some fluorinated substances bioaccumulate preferentially in storage lipids. The present work builds on this initial finding by characterizing EOF in an additional 3 killer whales (2 from Greenland, 1 from Sweden), and then subjecting extracts from all 4 whales to analysis via gas chromatography-atmospheric pressure chemical ionization-ion mobility mass spectrometry. Using collision cross sections, we prioritized features suspected to be highly fluorinated, and then selected 5 for manual annotation. Custom synthesised standards confirmed 10:2 and 12:2 fluorotelomer methylsulfone, 10:2 and 12:2 fluorotelomer chloromethylsulfone, and 6:2 bisfluorotelomer sulfone in all blubber samples from Greenland at concentrations ranging from <0.4-72.5 ng/g, explaining 34-75% of blubber EOF. None of these substances were observable in liver, suggesting preferential accumulation in storage lipids. To the best of our knowledge, this is the first report of fluorotelomer sulfones in wildlife and the first observation of lipophilic, highly fluorinated PFAS.

## Keywords

Combustion ion chromatography, gas chromatography ion mobility mass spectrometry, marine mammals, dolphins, cetaceans, non-target screening, PFAS

## Synopsis

Five novel fluorotelomer sulfones were identified in killer whales from Greenland, explaining up to 75% of extractable organofluorine in blubber. Their absence in liver points to their lipophilic nature, marking the first report of such compounds in wildlife.

## Introduction

Chemicals containing fully fluorinated methyl ( $-\text{CF}_3$ ) or methylene ( $-\text{CF}_2-$ ) groups are classified as per- and polyfluoroalkyl substances (PFAS).<sup>1</sup> These compounds, primarily of anthropogenic origin, find widespread use in both industrial and consumer applications.<sup>2</sup> To date, over 10 000 PFAS are known to exist on the global market, spanning both low-molecular weight water soluble substances, to high molecular weight, hydrophobic polymers.<sup>1</sup>

Most research on PFAS has focused on perfluoroalkyl acids (PFAAs) and their precursors. Among the most notorious PFAAs are perfluorooctane sulfonate (PFOS) and perfluorooctanoate (PFOA), highly water-soluble surfactants that possess very low  $\text{pK}_{\text{a}}$ s and tend to accumulate in protein- and phospholipid-rich tissues (such as liver and blood) rather than storage lipids (adipose tissue) like other persistent organic pollutants.<sup>3–5</sup> While PFAA-precursors and alternatives (e.g. perfluorooctane sulfonamide and perfluorinated ether acids, respectively) have a greater propensity for fat partitioning compared to PFAAs, their concentrations in storage lipids are usually much lower than those in liver or blood.<sup>4,6,7</sup> For other PFAS, particularly neutral substances, tissue-specific accumulation remains either unexplored or is assumed to follow behaviour similar to PFAAs. However, the impact of fluorination on lipophilicity is not always predictable. For instance, fluorination of an aromatic ring with either a single fluorine atom or a perfluoroalkyl group has been observed to increase lipophilicity compared to hydrogen at the same position, while fluorination of alkyl groups can lead to an increase or decrease in lipophilicity.<sup>8,9</sup>

Recently, our research group provided the first empirical evidence of large quantities of unidentified extractable organic fluorine (EOF) in the blubber of a marine mammal.<sup>7</sup> In that work, a combination of combustion ion chromatography (CIC) and mass spectrometry-based target analyses were applied to eight different tissues of a killer whale (*Orcinus orca*) from East Greenland. While the distribution of known PFAS in tissues aligned with previous findings (with decreasing concentrations in the order: liver > blood > kidney  $\approx$  lung  $\approx$  ovary > muscle  $\approx$  skin  $\approx$  blubber), unknown EOF concentrations determined via CIC were highest in blubber. These results could not be explained by inorganic fluorine (which was removed during the extraction procedure) or targeted PFAS. Considering that blubber can account for up to 50% of the entire body mass of some species of cetaceans at certain life stages,<sup>10,11</sup> we posit that overlooking chemicals in this compartment may significantly underestimate overall exposure to organofluorine substances.<sup>12</sup>

Efforts to characterize unidentified EOF have generally relied on suspect and non-target screening using liquid chromatography-high resolution mass spectrometry (LC-HRMS) with electrospray ionization (ESI).<sup>13–16</sup> This approach favours polar, charged, or easily ionizable compounds, and is generally unsuitable for non-polar/neutral substances, which do not ionize efficiently in ESI. To address this, a number of new methods have been developed based on gas chromatography-atmospheric pressure

chemical ionization-high resolution mass spectrometry (GC-APCI-HRMS), which have proven effective at uncovering novel non-polar PFAS in a wide range of matrices.<sup>17–20</sup> APCI is a softer ionization process compared to the traditionally used electron ionization (EI) in GC analyses, resulting in the detection of (quasi-)molecular ions. Additionally, when coupled with ion mobility spectrometry (IMS), collision cross sections (CCSs) can be used as an additional prioritization strategy for fluorinated substances.<sup>17</sup>

In this work we build on the initial discovery of unidentified EOF in the blubber of a Greenland killer whale by characterizing EOF in the blubber of 3 additional individuals, and then identifying the nature of this EOF using GC-APCI-IMS. To the best of our knowledge, this is the first study to identify lipophilic PFAS in wildlife.

## Materials and Methods

### Sample Collection

Blubber from three killer whales referred to herein as KW-16, KW-17 (previously characterized by Schultes et al. 2020),<sup>7</sup> and KW-20 were collected together with local subsistence Inuit hunters in 2016, 2017 and 2020, respectively, in Greenland. Liver was also obtained from KW-17. Blubber from a fourth killer whale (KW-23) which was found dead at Hunnebostrand, Sweden, in 2023, was also sampled. Further information on these samples, including CITES (Convention on International Trade in Endangered Species) permit numbers, can be found in Table S 1.

### Sample preparation

*Extraction.* Subsamples (2 g) of blubber (n=3 for KW-17; n=1 for all others) and liver (KW-17 only; n=2) were thawed at room temperature and then extracted with 4 mL of acetonitrile together with bead blending (10 minutes, 1500 rpm, SPEX SamplePrep 1600 MiniG®). Subsequently, the samples were centrifuged (Centrifuge 5810, Eppendorf), and the resulting supernatant was transferred to a new tube. The extraction process was repeated, and the supernatants were combined and concentrated down to 1 mL using a TurboVap LV Evaporator (Biotage). A portion of extract was removed for EOF determination.

*Lipid removal.* In preparation for characterization by GC-APCI-IMS, extracts were subjected to a lipid removal procedure, described elsewhere and adapted here.<sup>21</sup> Briefly, extracts were placed in a freezer (-24 °C) for 30 minutes to precipitate lipids. Thereafter the supernatants were filtered using a nylon syringe filter and the filtrates were placed in a new tube. The procedure was repeated on precipitated lipids once more using 2 mL of acetonitrile, and the filtrates were combined.

*Ion exchange clean-up.* We hypothesised that lipophilic organofluorines would be neutral, and therefore sought to reduce the complexity of extracts by removing substances with ionizable functional groups. This was achieved using a series of clean-up steps based on ion exchange SPE. Strong cation exchange cartridges (Oasis® MCX, 150 mg) were primed with 8 mL acetonitrile, extracts (~3 mL) were loaded and the cartridges were rinsed with an additional 8 mL of acetonitrile. The combined load and rinse were collected into a single polyethylene tube and reduced to ~3 mL by drying. This procedure was then repeated with strong anion exchange cartridges (Oasis® MAX, 150 mg). The final extracts were dried to ~0.1 mL and transferred to microvials for GC-APCI-IMS analysis.

*Quality control.* Method blanks for both EOF and GC-APCI-IMS analyses were determined by carrying out the same extraction procedure in empty tubes. In addition, portions of extract from KW-17 were retained after lipid removal and again after ion exchange clean-up. Analysis of these extracts by CIC revealed that EOF concentrations remained stable with each successive step, indicating that the major fluorinated substances in blubber were not inadvertently removed during clean-up. Instrumental QC procedures are described in the instrumental analysis section.

## **Instrumental analysis**

### ***Extractable Organofluorine analysis***

For EOF determination by CIC, extracts (100 µL) were loaded into prebaked ceramic sample boats containing glass wool. The samples were combusted at 1100 °C with oxygen (400 mL/min), argon (200 mL/min), and an argon/water vapor mix (100 mL/min) within the combustion unit (HF-210, Mitsubishi) for five minutes. During the combustion process, combustion gases were absorbed in Milli-Q water using a gas absorber unit (GA-210, Mitsubishi), they were subsequently separated and analysed using an ion-chromatograph (Dionex, Thermo Scientific). Quantification was accomplished using calibration points at 0.05, 0.1, 0.25, 0.5, 1, 5 and 10 ppm of NaF solution, employing an unweighted linear calibration curve. Analysis of a certified reference material (fluorine in clay,  $568 \pm 60$  µg F/g, n=3) and a solution of PFOS and PFOA (0.74 ng F/µL) were used to check for combustion efficiency throughout the run, resulting in recoveries of  $90\% \pm 9\%$  and  $105\% \pm 2\%$ , respectively. Mean fluoride concentrations from procedural blanks was subtracted from samples before quantification. The limit of quantification (LOQ; 33 ng F/g) was calculated using the average F concentration from procedural blanks plus 3 times the standard deviation of replicate blank measurements, and the average extract volume and sample weight.

## GC-APCI-IMS

Putative identification of fluorinated substances in KW-17 blubber extracts was carried out at Memorial University (Newfoundland, Canada), using an existing GC-APCI-IMS method for non-target discovery of halogenated substances.<sup>17</sup> These results were later replicated and built upon at Stockholm University using a recently developed GC-APCI-IMS method with few modifications.<sup>20</sup> Briefly, extracts (1  $\mu$ L) were injected onto an Agilent GC using pulse splitless mode with a programmed inlet temperature (i.e., initially 100 °C for 0.15 min, increased at 600 °C min<sup>-1</sup> to 280 °C, hold for 1 min). Analytes were separated on a 30-m DB-5MS Ultra Inert column (i.d., 0.25 mm; film thickness, 0.25  $\mu$ m; Agilent Technologies) with helium carrier gas at a constant flow of 1.5 mL min<sup>-1</sup>. The GC oven temperature program was as follows: hold at 70 °C for 1 min; increase at 10 °C min<sup>-1</sup> to 310 °C, then hold for 15 min (total run time=40 min). The GC was coupled via an APCI source to a Waters Select Series Cyclic IMS operated in positive ionization mode and under wet conditions (an open vial containing water was placed in the source and left to equilibrate overnight). The transfer line and ion source were maintained at 290 °C and 150 °C, respectively. The corona discharge needle and cone voltage were set at 2  $\mu$ A and 30 V, respectively. Nitrogen was used for the makeup-, auxiliary-, and cone gas at flow rates of 200 mL min<sup>-1</sup>, 150 L h<sup>-1</sup>, and 200 L h<sup>-1</sup>, respectively, under wet conditions. The MS was operated in the high-definition MS<sup>E</sup> mode with the mass range of 100-1200 amu. The collision energy was fixed at 6 eV at the low energy mode, and ramped between 15-50 eV at the high energy mode. The scan time was 0.3 s for each mode. The cyclic ion mobility cell was operated in the one pass mode with 5 pushes per bin at a traveling wave height of 15 V. Both drift gas and collision gas were nitrogen. Column bleeding (C<sub>9</sub>H<sub>27</sub>O<sub>5</sub>Si<sub>5</sub><sup>+</sup>;  $m/z$  355.0705) was measured every 2 min for internally mass calibration. CCS was calibrated using a mixture of 22 compounds supplied by Waters Corp. according to its standard procedure.

## Data Analysis

Lockmass correction, peak picking (minimum absolute ion intensity 40), run alignment, calculation of CCS measurements, and pairing of precursor and product ions (minimum 1% of parent ion) were carried out using Progenesis QI (version 3, Waters corporation). Peaks with areas at least 3 times higher than the area in the procedural blanks were kept for screening. Features were selected for further investigation if their CCS values were between 150 and 250 Å<sup>2</sup> and were lower than one fifth of their  $m/z + 100$  Å<sup>2</sup>, an approach previously demonstrated to be effective for prioritizing fluorinated substances.<sup>17</sup> The resulting features were further prioritized based on a) exact masses >400 Da (which we posited could serve as a threshold for bioaccumulative PFAS, given that long chain PFAAs have masses exceeding 400 Da), and b) mass defects between -0.1 and +0.05 (characteristic of highly fluorinated substances).<sup>22</sup> Finally, we prioritized the most intense features for manual inspection and annotation. Custom

synthesised standards for putatively identified compounds were purchased from Chiron AS (Trondheim, Norway) and used for confirmation and quantification.

## Quantification

Areas for quantification were obtained via Waters UNIFI™ software. Concentrations and matrix effects for identified PFAS in KW-17 were calculated by standard addition. For the other killer whales, semi-quantification was performed using an external one-point calibration (500 ng/mL mixture of the five fluorotelomer sulfones) and concentrations were adjusted by the matrix effect factor calculated in KW-17. Concentrations of measured PFAS (in ng/g) were converted to corresponding fluorine equivalent concentrations (i.e. ng F/g) and summed in order to compare with EOF measurements (details in the SI). LOQs were based on the analysis of the 500 ng/mL mixture: the equivalent concentration in ng/mL of a peak with height of 500 was calculated for each fluorotelomer sulfone and adjusted by their respective matrix effect factor. LOQs in samples (ng/g) were calculated using the average extract volume and average sample weight and are reported in Table S 2.

## Results and discussion

### EOF determination

EOF was measured in blubber of KW-16 (69 ng F/g, n=1), KW-17 (162±94 ng F/g, n=6) and KW-20 (82 ng F/g, n=1), while it was below limit of quantification for KW-23 (Figure 1, panel A). The EOF concentration in KW-17 reported here represents the triplicate measurement in this study combined with previous measurements by Schultes et al. (2020).<sup>7</sup> Measurement of EOF after clean-up (EnviCarb) in Schultes et al. and before any clean-up steps in the present work may explain the slight discrepancy in EOF concentrations between the two studies. The low level in KW-23 could be associated with its geographical location (Sweden), a different diet compared to the other killer whales, or the state of the animal, whose blubber appeared less dense in fats and had a higher relative proportion of connective tissue, suggesting that it may have died of starvation.

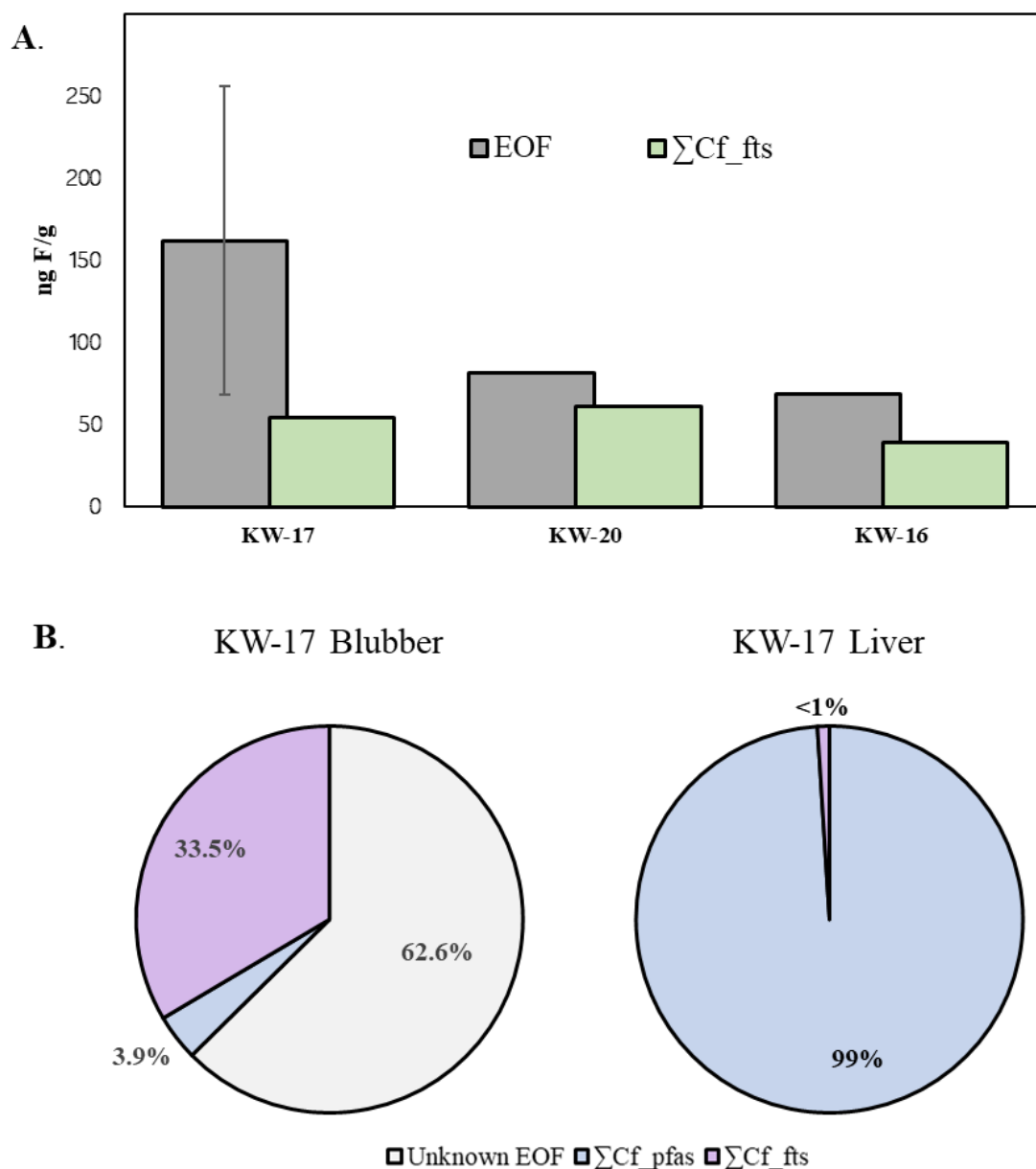


**Figure 1.** *Panel A*-EOF (grey) and  $\sum C_{F\_FTS}$  (sum of concentrations of fluorotelomer sulfones in fluorine equivalents, green) in ng F/g, measured in the blubber of killer whales. *Panel B*-percentage of EOF in blubber and liver of KW-17 explained by  $\sum C_{F\_PFAS}$  (in blue, the sum of concentrations of PFAS measured by LC-HRMS by Schultes et al. (2020), in F equivalents) and  $\sum C_{F\_FTS}$  measured by GC-MS in this study (purple), along with remaining unidentified EOF (light grey). In the liver,  $\sum C_{F\_FTS}$  concentrations were estimated using their LOQs, resulting in a value that is less than 1% of the EOF.



## 216 HRMS characterization

217 A total of 32343 features ( $>3\times$  the abundance in method blanks) were observed in the KW-17 extract  
 218 prior to any prioritization steps. Application of the CCS prioritization reduced the total number of  
 219 features to 4748, which was further reduced to 478 features by selecting masses  $>400$  Da which also  
 220 displayed a mass defect between  $-0.1$  and  $+0.05$ . Features were then ordered by intensity, and 5 were  
 221 selected for structural elucidation (Figure 2).

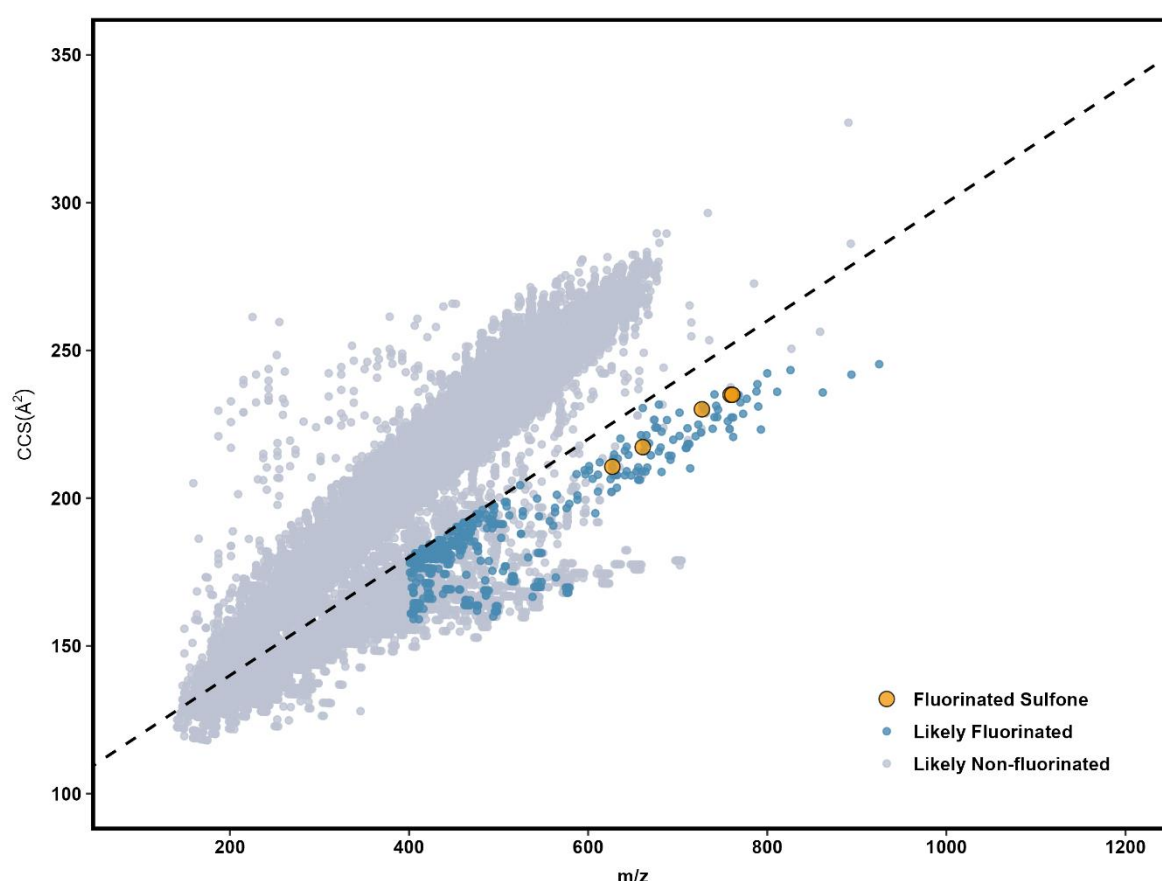


**Figure 2.** Plot of mass-to-charge ratios ( $m/z$ ) versus collision cross section (CCS) of peaks detected in KW-17. Peaks with a CCS value under the threshold ( $100\text{\AA}^2 + 0.2 \times m/z$ ; denoted by the dashed line) were prioritized as potential halogenated compounds. Further prioritization as possible fluorinated substances (in blue) utilized criteria of  $m/z > 400$ , and mass defect between  $-0.1$  and  $+0.05$ . Identified features (the five fluorotelomer sulfones) are in orange.

222 The two most abundant peaks ( $m/z$  627 and 727), were putatively identified as protonated ions of 10:2  
 223 fluorotelomer methylsulfone (10:2 FTSO<sub>2</sub>Me;  $[\text{C}_{13}\text{H}_8\text{F}_{21}\text{SO}_2]^+$ ) and 12:2 fluorotelomer methylsulfone  
 224 (12:2 FTSO<sub>2</sub>Me;  $[\text{C}_{15}\text{H}_8\text{F}_{25}\text{SO}_2]^+$ ). Inspection of the product ion spectra for  $m/z$  627 and 727 (Figure S1)

revealed loss of HF, producing fragments  $[C_{13}H_7F_{20}SO_2]^+$  and  $[C_{15}H_7F_{24}SO_2]^+$ , respectively, and subsequent loss of  $SO_2CH_4$ , forming fragments  $[C_{12}F_{20}H_3]^+$  and  $[C_{14}F_{24}H_3]^+$ , respectively. From these, subsequent fragmentation follows either loss of  $C_2H_2$  and another HF giving fragments  $[C_{10}F_{19}]^+$  and  $[C_{12}F_{23}]^+$ , respectively, or loss of  $CHF_3$  resulting in fragments  $[C_{10}F_{17}CH_2]^+$  and  $[C_{12}F_{21}CH_2]^+$ , respectively. Other smaller fluorinated fragments were also present in the product ion spectrum (Figure S 1).

Following putative identification of the methyl sulfones, 10:2 fluorotelomer chloromethylsulfone (10:2  $FTSO_2MeCl$ ) and 12:2 fluorotelomer chloromethylsulfone (12:2  $FTSO_2MeCl$ ) were tentatively identified at lower intensities. These substances were noticed because 10:2  $FTSO_2MeCl$  appeared to partially co-elute with 12:2  $FTSO_2Me$ . Fragmentation patterns followed loss of  $CH_3OCl$ , producing  $[C_{12}F_{21}H_4SO]^+$  and  $[C_{14}F_{25}H_4SO]^+$ , or loss of the sulfone chloromethyl head and HF, giving major fragments  $[C_{12}F_{20}H_3]^+$  and  $[C_{14}F_{24}H_3]^+$ , respectively. From these, additional fragmentation follows the same pattern as for  $FTSO_2Me$  (Figures S2 and S3).

The third most abundant peak after prioritisation was  $m/z$  759, which was putatively identified as 6:2 bisfluorotelomer sulfone (bis(6:2 FT) $SO_2$ ). Fragments observed in the product ion spectrum (Figure S4) are due to loss of HF  $[C_{16}F_{25}H_8SO_2]^+$ , loss of one of the fluorotelomer sulfone chains  $[C_8F_{13}H_6SO_2]^+$ , and a subsequent loss of HF, giving fragment  $[C_8F_{12}H_5SO_2]^+$  which is itself followed by loss of  $S(OH)_2$  resulting in  $[C_8F_{12}H_3]^+$ .

Increasing retention times and CCS values for the two sets of homologues, as well as observation of all five compounds in a similar region of the chromatogram increased confidence in the structural assignment and custom-made analytical standards were purchased from Chiron for confirmation and quantification. Details on the fluorotelomer sulfones structure,  $m/z$ , retention times and CCS values can be found in Table 1.

### Confirmation, quantification and organofluorine mass balance

Analysis of custom synthesised standards confirmed the identities of the five fluorotelomer sulfones in KW-17 at a sum concentration ( $\sum C_{FTS}$ ) of 83.9 ng/g, made up of 23.6 ng/g 10:2  $FTSO_2Me$ , 55.2 ng/g 12:2  $FTSO_2Me$ , 1.1 ng/g 10:2  $FTSO_2MeCl$ , 0.4 ng/g 12:2  $FTSO_2MeCl$  and 3.6 ng/g bis(6:2 FT) $SO_2$ . These targets were not observable in liver from the same animal. Subsequent analysis in the additional killer whales revealed similar sum concentrations to KW-17 for both KW-16 (60.3 ng/g) and KW-20 (94.0 ng/g), with 12:2  $FTSO_2Me$  displaying the highest concentrations, followed by 10:2  $FTSO_2Me$ , bis(6:2 FT) $SO_2$  and 10:2  $FTSO_2MeCl$ . For 10:2  $FTSO_2MeCl$ , peaks were detectable but areas were below LOQ. KW-23 was the only animal where these targets were not observed. Detailed concentrations can be found in Table S 2.

Conversion of  $\sum C_{\text{FTS}}$  to fluorine equivalents ( $\sum C_{\text{F-FTS}}$ ) revealed concentrations of 39.2, 54.4, and 61.2 ng F/g, for KW16, 17, and 20, accounting for 57%, 34%, and 75% of the EOF in these animals, respectively. Schultes et al.<sup>7</sup> previously measured a suite of polar PFAS by LC-HRMS in KW-17 blubber extracts, which accounted for only 6.3 ng F/g (4% of EOF). When combined with fluorotelomer sulfone concentrations, 37% of EOF was explained in KW-17 blubber (Figure 1, panel B), suggesting that additional fluorinated compounds still remain to be identified in blubber. In comparison, if we hypothesise that these compounds are present in the liver at their LOQs, they would correspond to <1% of the EOF, with the balance closed by polar PFAS (Figure 1B).

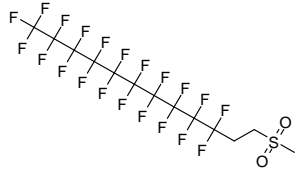
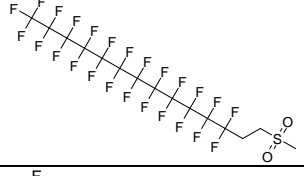
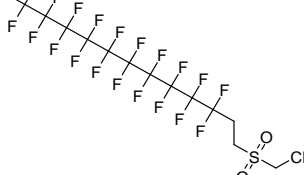
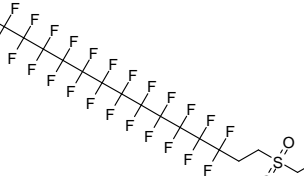
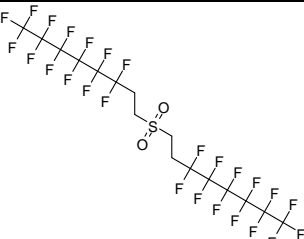
## Implications

To the best of our knowledge, this is the first report of highly fluorinated non-polar PFAS in the blubber of marine mammals. Fluorinated liquid crystal monomers (LCMs) have been observed in the blubber of Indo-Pacific humpback dolphins; however, these are structurally different from the substances observed here, possessing a biphenyl backbone structure and fewer fluorine atoms.<sup>23</sup> Our group has subsequently observed n:2 FTSO<sub>2</sub>Me (n=8, 10, 12, 14) in sediment samples from the Baltic sea, the Arctic, a Norwegian lake contaminated with PFAS from a paper production facility, and NIST standard reference material (1941b-Organics in Marine Sediment).<sup>20</sup> The 10:2 FTSO<sub>2</sub>Me and shorter-chain homologues of the same class, 6:2 and 8:2, have been tentatively observed in a waste water treatment plant influent from Spain.<sup>18</sup>

The occurrence of these chemicals in blubber of several killer whales sampled in Greenland indicates that they are subject to long-range transport but exhibit novel bioaccumulative behaviour since they were not observed in liver, thus challenging the paradigm that all PFAS bioaccumulate through interactions with proteins or phospholipids. Notably, since the blubber can constitute up to 50% of body weight in whales,<sup>11</sup> fluorotelomer sulfones might represent a significantly higher body burden for these animals compared to the polar PFAS found in the liver (2-3% of body weight in mammals).<sup>24</sup>

Given that a considerable portion of EOF remains unexplained and more than 450 features prioritized as possible PFAS remain unidentified, further investigation is necessary. However, this study marks a significant advancement in understanding the composition of EOF in lipid-rich tissues and highlights the importance of including non-polar PFAS in fluorine mass balance studies and in environmental exposure considerations.

**Table 1-** Structures, names, and acronyms of the fluorotelomer sulfones, the formula and calculated  $m/z$  of  $[M+H]^+$ , the average ppm error of the observed  $m/z$  in the killer whales, the major product ions used for structural elucidation, the retention time (RT), the average CCS value in standard, and the average CCS relative deviation (%) in the killer whales. The high mass error (>5 ppm) in killer whales for 10:2 and 12:2 FTSO<sub>2</sub>Me was also observed in the analytical standards at high concentrations.

Structure	Name	$[M+H]^+$	$m/z$	$\Delta\text{ppm}$	Product ions	RT	CCS	$\Delta\text{CCS}(\%)$
	10:2 fluorotelomer methylsulfone (10:2 FTSO <sub>2</sub> Me)	$[C_{13}H_8F_{21}SO_2]^+$	626.9904	6.50	606.9842 $[C_{13}F_{20}H_7SO_2]^+$ , 526.9910 $[C_{12}F_{20}H_3]^+$ , 480.9691 $[C_{10}F_{19}]^+$ , 456.9880 $[C_{10}F_{17}CH_2]^+$	10.49	210.03	0.85
	12:2 fluorotelomer methylsulfone (10:2 FTSO <sub>2</sub> Me)	$[C_{15}F_{25}H_8SO_2]^+$	726.98403	5.54	706.9778 $[C_{15}F_{24}H_7SO_2]^+$ , 626.9846 $[C_{14}F_{24}H_3]^+$ , 580.9627 $[C_{12}F_{23}]^+$ , 556.9816 $[C_{12}F_{21}CH_2]^+$	11.65	230.48	0
	10:2 fluorotelomer chloromethylsulfone (10:2 FTSO <sub>2</sub> MeCl)	$[C_{13}H_7ClF_{21}SO_2]^+$	660.951446	3.61	594.9642 $[C_{12}F_{21}H_4SO]^+$ , 526.9910 $[C_{12}F_{20}H_3]^+$ , 480.9691 $[C_{10}F_{19}]^+$ , 456.9880 $[C_{10}F_{17}CH_2]^+$	11.66	217.65	0.78
	12:2 fluorotelomer chloromethylsulfone (12:2 FTSO <sub>2</sub> MeCl)	$[C_{15}H_7ClF_{25}SO_2]^+$	760.94506	3.24	694.9578 $[C_{14}F_{25}H_4SO]^+$ , 626.9846 $[C_{14}F_{24}H_3]^+$ , 580.9627 $[C_{12}F_{23}]^+$ , 556.9816 $[C_{12}F_{21}CH_2]^+$	12.77	236.51	0.69
	6:2 bisfluorotelomer sulfone (Bis(6:2 FT)SO <sub>2</sub> )	$[C_{16}H_9F_{26}SO_2]^+$	758.99026	3.80	738.98403 $[C_{16}F_{25}H_8SO_2]^+$ , 412.9875 $[C_8F_{13}H_6SO_2]^+$ , 392.9813 $[C_8F_{12}H_5SO_2]^+$ , 327.0038 $[C_8F_{12}H_3]^+$	10.24	235.34	0.95

## Associated content

Details on chemicals, reagents, and data handling. MS/MS figures of the five fluorotelomer sulfones, table with information on killer whales sampled, and table detailing measured concentrations of fluorotelomer sulfonates and extractable organofluorine.

## Acknowledgments

This project has received funding from the European Union's Horizon 2020 research and innovation programme under Marie Skłodowska-Curie Action Grant Agreement 860665. XS acknowledges funding from the Marie Skłodowska-Curie postdoctoral fellowship under Horizon Europe (Grant agreement number: 101150779). We thank the Indigenous hunters in Tasiilaq, who helped us sample their catch. The sampled animals are part of the legal indigenous subsistence hunt. The collection of samples from Greenland was funded by the Ministry of Environment of Denmark (#MST-113-00054).

## References

1. OECD. *Reconciling Terminology of the Universe of Per- and Polyfluoroalkyl Substances*. Vol 61. (OECD Series on Risk Management, ed.). OECD; 2021. doi:10.1787/e458e796-en
2. Glüge J, Scheringer M, Cousins IT, et al. An overview of the uses of per- and polyfluoroalkyl substances (PFAS). *Environ Sci Process Impacts*. 2020;22(12):2345-2373. doi:10.1039/D0EM00291G
3. Ng CA, Hungerbühler K. Bioaccumulation of Perfluorinated Alkyl Acids: Observations and Models. *Environ Sci Technol*. 2014;48(9):4637-4648. doi:10.1021/es404008g
4. Dassuncao C, Pickard H, Pfohl M, et al. Phospholipid Levels Predict the Tissue Distribution of Poly- and Perfluoroalkyl Substances in a Marine Mammal. *Environmental Science & Technology Letters*. 2019;6(3):119-125. doi:10.1021/acs.estlett.9b00031
5. Ng CA, Hungerbühler K. Bioconcentration of Perfluorinated Alkyl Acids: How Important Is Specific Binding? *Environ Sci Technol*. 2013;47(13):7214-7223. doi:10.1021/es400981a

6. Robuck AR, McCord JP, Strynar MJ, Cantwell MG, Wiley DN, Lohmann R. Tissue-Specific Distribution of Legacy and Novel Per- and Polyfluoroalkyl Substances in Juvenile Seabirds. *Environ Sci Technol Lett.* 2021;8(6):457-462. doi:10.1021/acs.estlett.1c00222
7. Schultes L, van Noordenburg C, Spaan KM, et al. High Concentrations of Unidentified Extractable Organofluorine Observed in Blubber from a Greenland Killer Whale (*Orcinus orca*). *Environ Sci Technol Lett.* 2020;7(12):909-915. doi:10.1021/acs.estlett.0c00661
8. Jeffries B, Wang Z, Felstead HR, et al. Systematic Investigation of Lipophilicity Modulation by Aliphatic Fluorination Motifs. *J Med Chem.* 2020;63(3):1002-1031. doi:10.1021/acs.jmedchem.9b01172
9. Glyn RJ, Pattison G. Effects of Replacing Oxygenated Functionality with Fluorine on Lipophilicity. *J Med Chem.* 2021;64(14):10246-10259. doi:10.1021/acs.jmedchem.1c00668
10. Perrin WF, Wursig B, Thewissen JGM. *Encyclopedia of Marine Mammals*. Elsevier; 2009. doi:10.1016/B978-0-12-373553-9.X0001-6
11. Lockyer C. Body weights of some species of large whales. *ICES Journal of Marine Science.* 1976;36(3):259-273. doi:10.1093/icesjms/36.3.259
12. Plön S, Andra K, Auditore L, et al. Marine mammals as indicators of Anthropocene Ocean Health. *npj Biodiversity.* 2024;3(1):24. doi:10.1038/s44185-024-00055-5
13. Haque F, Soerensen AL, Sköld M, et al. Per- and polyfluoroalkyl substances (PFAS) in white-tailed sea eagle eggs from Sweden: temporal trends (1969–2021), spatial variations, fluorine mass balance, and suspect screening. *Environ Sci Process Impacts.* 2023;25(9):1549-1563. doi:10.1039/D3EM00141E
14. Spaan KM, van Noordenburg C, Plassmann MM, et al. Fluorine Mass Balance and Suspect Screening in Marine Mammals from the Northern Hemisphere. *Environ Sci Technol.* 2020;54(7):4046-4058. doi:10.1021/acs.est.9b06773
15. Cioni L, Nikiforov V, Benskin JP, et al. Combining Advanced Analytical Methodologies to Uncover Suspect PFAS and Fluorinated Pharmaceutical Contributions to Extractable

- Organic Fluorine in Human Serum (Tromsø Study). *Environ Sci Technol.* 2024;58(29):12943-12953. doi:10.1021/acs.est.4c03758
16. Lauria MZ, Sepman H, Ledbetter T, et al. Closing the Organofluorine Mass Balance in Marine Mammals Using Suspect Screening and Machine Learning-Based Quantification. *Environ Sci Technol.* 2024;58(5):2458-2467. doi:10.1021/acs.est.3c07220
  17. MacNeil A, Li X, Amiri R, et al. Gas Chromatography-(Cyclic) Ion Mobility Mass Spectrometry: A Novel Platform for the Discovery of Unknown Per-/Polyfluoroalkyl Substances. *Anal Chem.* 2022;94(31):11096-11103. doi:10.1021/acs.analchem.2c02325
  18. Portolés T, Rosales LE, Sancho J V, Santos FJ, Moyano E. Gas chromatography-tandem mass spectrometry with atmospheric pressure chemical ionization for fluorotelomer alcohols and perfluorinated sulfonamides determination. *J Chromatogr A.* 2015;1413:107-116. doi:10.1016/j.chroma.2015.08.016
  19. Shi X, Sobek A, Benskin JP. Multidimensional-constrained Suspect Screening of Hydrophobic Chemicals Using Gas Chromatography-Atmospheric Pressure Chemical Ionization-Ion Mobility-Mass Spectrometry. Published online October 25, 2024. doi:10.26434/chemrxiv-2024-hscrk
  20. Shi X, Langberg HA, Sobek A, Benskin JP. Exploiting Molecular Ions for Screening Hydrophobic Contaminants in Sediments using Gas Chromatography-Atmospheric Pressure Chemical Ionization-Ion Mobility-Mass Spectrometry. Published online October 28, 2024. doi:10.26434/chemrxiv-2024-ft9cl
  21. Hong J, Kim HY, Kim DG, Seo J, Kim KJ. Rapid determination of chlorinated pesticides in fish by freezing-lipid filtration, solid-phase extraction and gas chromatography-mass spectrometry. *J Chromatogr A.* 2004;1038(1-2):27-35. doi:10.1016/J.CHROMA.2004.03.003
  22. Liu Y, D'Agostino LA, Qu G, Jiang G, Martin JW. High-resolution mass spectrometry (HRMS) methods for nontarget discovery and characterization of poly- and per-fluoroalkyl substances (PFASs) in environmental and human samples. *TrAC Trends in Analytical Chemistry.* 2019;121:115420. doi:10.1016/j.trac.2019.02.021

23. Tao D. *Investigation of Occurrence, Sources, Transport, and Preliminary Environmental Risk of Liquid Crystal Monomers in the South China Sea Area*. PhD thesis. City University of Hong Kong; 2024.
24. Prothero JW. Organ scaling in mammals: The liver. *Comp Biochem Physiol A Physiol*. 1982;71(4):567-577. doi:10.1016/0300-9629(82)90205-5